Ionic Conductivity in Disordered Media: Molecular Flexibility as a New Paradigm to Enhance Ion Motion in Glassy Electrolytes

M. Micoulaut
Sorbonne Université, Laboratoire de Physique Théorique de la Matière Condensée, CNRS UMR 7600, 4 Place Jussieu, 75252 Paris Cedex 05, France

(Received 27 November 2023; revised 21 March 2024; accepted 22 November 2024; published 23 January 2025)

We investigate the role of molecular flexibility on the electrical transport properties of model electrolytes containing ions and an underlying disordered network structure with changing connectedness. Rather than focusing on the effect of ion content in a stoichiometric network former AY_2 (e.g., SiS_2), we explore the possibility of increasing the Y:A ratio (flexibility index m) in order to reduce connectivity and to promote the occurrence of flexible modes and topological degrees of freedom in the network structure. At fixed ion content and below a certain threshold modifier composition x_c, topological constraint counting indicates that a mean-field stress-to-flexible transition is expected for a flexibility index m_c, and an ion hopping model predicts a substantial increase of conductivity once $m > m_c$. Molecular dynamics simulations on a typical amorphous electrolyte, $x\mathrm{Na_2S} - (1-x)\mathrm{SiS}_m$, independently and quantitatively confirm the prediction as anomalous changes with m are obtained, and these manifest by waterlike diffusivity anomalies, and a substantial increase of ionic conductivity upon moderate change of m. The analysis disentangles contributions from mobility and the free carrier rate in the electrical transport, and finally suggests that molecular flexibility can serve as an efficient way for conductivity enhancement in all solid-state batteries using amorphous electrolytes.

DOI: 10.1103/PhysRevLett.134.036303

The worldwide ubiquitous use of portable electronics and their increasing demands for energy and power, as for example in laptop computers and smartphones in use today, has exploded the demand for higher energy and power density batteries [1]. A promising perspective builds on the use of glasses which can serve as solid electrolytes and solve critical safety problems in dedicated all solid-state batteries. Key research topics for the improvement of the performance of amorphous electrolytes have focused on the role of the glassy matrix that needs to be established, and the role of migrating ions such as $Li^{\oplus}$ whose limited mineral resources also represent an issue of crucial importance. In order to bring such grand challenges to the next level, there is a need to find physical theory guided new strategies for conduction enhancement [2].

The question of transport phenomena (diffusion, conductivity) has often been addressed within the framework of percolation theory [3] which can be readily used on regular lattices by focusing on the percolation of sites or bonds representing moving charge carriers. This is a rather standard problem in statistical and computational physics. In disordered systems such as glasses or amorphous solids, the question of defining periodic hopping sites for an efficient mathematical treatment is hopeless, and additional features specific to such materials must be taken into account such as the presence of voids [4], spatially disordered conductive channels and their possible percolation under certain conditions [5], and, more generally, the possibility to have a variety of sites with a given structural information that produce select diffusion pathways [6]. Clearly, the overall properties of the host network with its disordered character must impact such transport phenomena.

In glasses which are disordered materials, an experimental standard route is to focus on compositional trends with the alkali content x of electrical properties in chalcogenide glasses [7,8], in relationship with physical and chemical properties. Compared to their oxide counterparts, these have superior ionic conductivities at room temperature (up to $\simeq 10^{-3}\ \Omega^{-1}\,\mathrm{cm}^{-1}$ [9]) and can be formed more easily due to lower glass transition temperatures. However, rather than following this standard strategy by investigating with ion content alone a given family of glasses with a stoichiometric network former (e.g., P_2S_5 in popular $(1-x)P_2S_5 - xLi_2S$ electrolytes [10]), an original and slightly different approach can be adopted by targeting the notion of flexibility for conductivity (σ) enhancement. It is well-known [11] that flexible (or low energy deformation) modes are present in sulphur-rich glasses such as P_xS_{1-x} with $x < \frac{2}{5}$. Alkali additives in off-stoichiometric glass formers, e.g., Si_xS_{100-x}, afford therefore, a unique venue for exploring new routes for an increase of conductivity in glassy electrolytes. Indeed, a natural guess is that once the glass network has lost its rigidity and becomes

flexible at the molecular level, it will contain an important fraction of low energy local deformation (flexible) modes which might promote the mobility of the charge carriers, and lead to a growth of conductivity σ.

In this Letter, we theoretically address the possibility to enhance ion motion by acting on the underlying network properties. A rigidity analysis is applied to a typical nonstoichiometric tetrahedral glass former AY_m (e.g., GeS_m) whose base network is disrupted by alkali ions M_2Y (e.g., Na_2S) [12]. Noteworthy is the fact that one considers $m \neq 2$, i.e., unlike GeS_2 there is the possibility to introduce at fixed modifier content x flexible (floppy) modes into the network by increasing the amount m of twofold Y (chalcogen) atoms. Once a Phillips-Thorpe topological constraint count is applied to the network, an isostatic condition is obtained at some threshold content m_c which is identified with the locus of a mean-field rigidity transition (MFRT). Within this framework inspired from Maxwell's pioneering study of the stability of trusses, atomic interactions are treated as mechanical constraints, and the resulting transition is of mean-field type as neither spatial fluctuations nor coordination defects are considered. It is shown that flexible networks satisfying $m > m_c$ display interesting properties regarding electrical transport. We then calculate from a phenomenological model [13] the ionic conductivity and identify distinct régimes for σ over identified flexible and stressed rigid topological phases. Such results are then enriched and brought to a more quantitative level from molecular dynamics simulations on a model $xNa_2S-(1-x)SiS_m$ system which exhibits for $m \geq 2$ a certain number of anomalies in transport properties close to m_c, in close connection with the salient phenomenology of glass or liquid rigidity [14]. While most if not all amorphous conductors use only stoichiometric compounds, this Letter opens a new window to tailor fast-ion transport, especially in sulfides which represent the most promising glassy materials for such applications [1]. Ultimately, it is expected to identify alternative alloying possibilities able to induce an increase of ionic conduction in amorphous electrolytes.

Our first piece of evidence builds on the approach developed by Mauro and co-workers [15,16] who use a constraint theory to model topological degrees of freedom in glasses with changing composition or connectivity, that we combine with a phenomenological conductivity model introduced for a silicate model structure [13]. For a modified tetrahedral network glass of the form $xM_2Y-(1-x)AY_m$ or $M_{2x}A_{1-x}Y_{m(1-x)+x}$ with, e.g., M = Li, Na; A = Si, Ge; and Y = S, Se, a $T=0$ mean-field constraint count [14] assuming the octet rule and broken bond-bending interactions [17] for so-called nonbridging sulfur (NBS) which are close to the alkali ions, leads to a fraction of topological degrees of freedom that is equal to

$$f = 3 - \frac{(1-x)(7+2m)+x}{1+2x+m(1-x)} \tag{1}$$

where the number of atoms in the network is derived from the chemical formula of the considered system, i.e., $N = 1+2x+m(1-x)$. Here Eq. (1) is obtained by assuming a disordered network constrained by bending and stretching interactions whose atomic density for an r-fold coordinated atom is given by $r/2$ and $(2r\text{-}3)$, respectively (see detail of the species contribution in Supplemental Material [18]). For example, the atom A contribution to the constraint density is $7(1-x)$. From Eq. (1), a MFRT satisfying $f=0$ is, thus, expected for the condition $m_c = (4-12x)/(1-x)$.

The local structure of the disordered network can be, furthermore, thought as a collection of three building blocks: $AY_{4/2}$ and $MAY_{5/2}$ tetrahedra, and a Y_2 chalcogen chain with probability p_4, p_3, and p_2, respectively. The latter element permits us to tune the connectivity of the base network [13] in the regime $m \geq 2$, whereas the $MAY_{5/2}$ unit contains a so-called nonbridging Y atom in the vicinity of the M cation (NBS in sulfides). One, furthermore has by virtue of probability conservation $p_4+p_3+p_2=1$, and from stoichiometry $p_4 = 2(1-3x)/m(1-x)$ and $p_3 = 4x/m(1-x)$. From all possible structural connections $j{-}k$ containing such basic building blocks $(j,k=2,3,4)$, we evaluate associated probabilities $p_{jk} \propto W_{jk}p_jp_k \exp[-E_{jk}/k_BT]$ and such connections $j{-}k$, and their corresponding energies can be classified [30] according to their rigidity status [flexible (FL), isostatic (IS), stressed rigid (SR) [18]]. Here W_{jk} represents an entropic factor, i.e., the number of equivalent ways to connect two species j and k together (e.g., $W_{43}=24$, see clusters displayed in Fig. 1), and E_{jk} represents an energy gain which depends on the elastic nature of the connection $j{-}k$: FL, IS, and SR. The density of topological degrees of freedom $f^{(2)}$ can then be calculated [15,16] from such connections according to

$$f^{(2)} = \sum_{j,k=FL} (3N_{jk} - N_{c(jk)}) N_{jk}^{-1} p_{jk} \tag{2}$$

where $N_{c(jk)}$ and N_{jk} are the number of topological constraints and the number of atoms found in a cluster $j{-}k$ with probability p_{jk}, respectively. Here, the sum runs only over flexible (FL) connections satisfying $N_{c(jk)} < 3N_{jk}$.

The profile of such probabilities p_{jk} with modifier content M_2Y appears in Figs. 1(a)–1(c) for select values of the flexibility index m. For the "stoichiometric" $m=2$, one recovers the usual evolution of rigidity loss, that is, a dominant stressed rigid network at low modifier content, typically $x < 15\%$ M_2Y (black curves), a growing fraction of isostatic clusters (cyan) with increasing x which

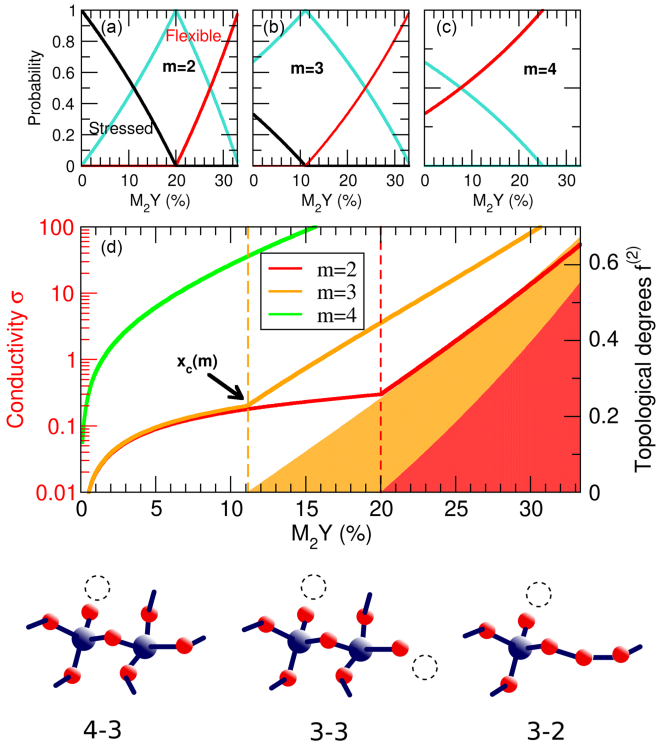

FIG. 1. (a)–(c) Probability of finding stressed (black), isostatic (cyan), and flexible (red) clusters for different flexibility indexs m as a function of modifier (M_2Y) content x: $m = 2$ (a), $m = 3$ (b) and $m = 4$ (c). (d) Calculated conductivity [Eq. (3)] for different m values (green, orange, red), and parameters $E_c = 0.0002$ and $\Delta = 0.2$ in k_BT units. The right axis represents the topological degrees of freedom [Eq. (2) for $m = 2$ (red) and $m = 3$ (orange)] as a function of x. The location $x_c(m)$ of the MFRT (broken vertical lines) is indicated for each m. Bottom: three clusters with respective probabilities $p_{43} \propto 24p_4p_3e_{\mathrm{IS}}$, $p_{33} \propto 9p_3^2e_{\mathrm{FL}}$ and $p_{32} \propto 12p_3p_2e_{\mathrm{FL}}$ (see full detail as a function of m and x in [18]), and anionic sites (circles with broken lines) that can be identified for the hopping model.

maximize around $x \simeq 20\%$ [Fig. 1(a)], consistently with the prediction of a MFRT at this composition [17], and with the experimental detection of an elastic threshold [31] for $M = \mathrm{Na}$, $Y = \mathrm{O}$, and $A = \mathrm{Si}$ (sodium silicates). With increasing m, the network connectivity and the constraint density now decrease, inducing a growth in topological degrees of freedom [$f^{(2)}$, Fig. 1(d), right axis] which become nonzero for $x_c(m) = (4 - m)/(12 - m)$, i.e., at the same condition as the one obtained for $f = 0$ in Eq. (1). As the index m and the overall network flexibility increase, the locus of the MFRT shifts to lower x, and for $m = 4$ this transition vanishes because the base network former [i.e., at $x = 0$] is already isostatically rigid (e.g., GeS_4 [32]), and any addition of alkali ions will further increase the network flexibility [red curve in Fig. 1(c)]. It is also interesting to note that the model is able to reproduce the salient features of rigidity transitions in Group IV chalcogenides with (i) a MFRT for random networks when $x = 0$, in absence of structural self-organization [14], (ii) for select (m, x) conditions a topological Boolchand phase [11,30,32] where the network remains essentially isostatic [18]. These features extracted from a simple model highlight the fact that close to the locus of the MFRT, a certain number of anomalies (extrema, thresholds) in physical properties should be expected [14], as discussed below.

Application of a hopping model [13] then permits us to calculate from the probabilities p_{jk} and Eq. (2) an ionic conductivity σ using mobility μ and free carrier rate n_L:

$$\sigma = n_L\mu = 2x\,\exp[-\langle E_c\rangle/k_BT].\exp[-E_m/k_BT] \quad (3)$$

with a Coulomb energy averaged over the various anionic sites [snapshots in Fig. 1(d)]:

$$\langle E_c\rangle = \sum_{j,k}\sum_{q} qE_cp_{jk}\exp[-qE_c/k_BT] \quad (4)$$

where E_c is the Coulombic energy to extract a single cation $M^{\oplus}$ from an anionic site and acts as a free parameter in the theory. $E_m = -\Delta f^{(2)}$ with $\Delta \simeq 5$ meV $= 0.2\ k_BT$ [33] is usually a strain energy that can be expressed as a function of the floppy mode density $f^{(2)}$, i.e., the network deformation energy E_m is favored if local (flexible) deformation modes are present.

Results for the conductivity are given in Fig. 1(d), and clearly suggest that the presence of flexible modes will substantially enhance ionic conduction. For $m = 2$ and with addition of an alkali modifier (M_2Y), the increase of $\sigma(x)$ is first driven by the growing presence of charge carriers (n_L), prior to a substantial increase once $f^{(2)} \neq 0$ at the threshold $x_c(m)$. The trend clearly indicates that the presence of network flexibility will enhance ionic conduction, and mimics the exponential evolution of conductivity during an intermediate to flexible transition [13]. At fixed alkali content x, an increase of the flexibility index m now induces a growth of σ by up to one order of magnitude (e.g., at $x = 20\%$, comparison between σ for $m = 2$ and $m = 3$).

Our second piece of evidence for conductivity enhancement driven by network flexibility uses molecular simulations which provide a support to the predicted thresholds, and lead to additional insight at the atomic scale, while also contrasting the results obtained from the simple hopping model. Here we work at fixed alkali content x on a $N = 3000$ particle system $(1 - x)SiS_m - xNa_2S$, and use a classical Born-Mayer (BM) force field that has been fitted [34] in order to simulate the structure of sodium thiosilicates. This potential is able to reproduce the main features of the structure factor $S(k)$ (position and amplitude of the main peaks) of the Na_2SiS_3 (NS) composition, as well as experimental data on diffusivity and conductivity for $m = 2$ [18]. The obtained structure is made of $SiS_{4/2}$

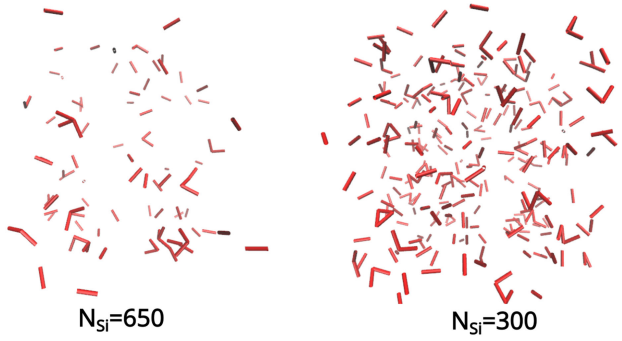

FIG. 2. Sulfur-related underlying network structure at 300 K in NS9 for $N_{\mathrm{Si}} = 650$ and $N_{\mathrm{Si}} = 300$ obtained from molecular dynamics simulations. Bars represent the homopolar S—S bonds which are absent for $N_{\mathrm{Si}} = 900$ ($m = 2$).

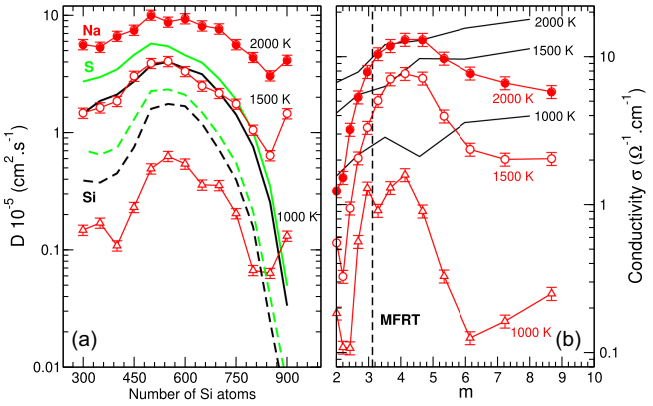

FIG. 3. (a) Calculated Na diffusivities (red) at 2000 K (filled circles), 1500 K (open circles), and 1000 K (open triangles) in NS9. Si (black) and S (green) diffusivities appear as solid and broken lines for 2000 K and 1500 K, respectively. (b) Calculated Nernst-Einstein conductivity σ as a function of the flexibility index m for different isotherms in NS9 (red) and NS (black). The vertical broken line indicates the locus of the MFRT in NS9. Error bars are of the order of the size of the symbols.

tetrahedra that are connected by corners and edges as also revealed from experiments [35]. The simulations provide, therefore, a good basis for further investigations, albeit obvious limitations can be expected as the BM parameters have been fitted only on the single NS composition so that inaccurate force-field effects might appear for any other (x, m) condition. But as we are seeking a generic effect, we work for this reason at fixed cell length in NVT by varying only the connectivity via the flexibility index m, and the subsequent induced homopolar S—S bond population (Fig. 2). With varying the flexibility index or sulfur content m, each starting system is cooled from a high temperature state (2500 K, atomic position memory loss) to different liquid target temperatures in NVT at which a clear diffusive regime can be found for $t < 100$ ps [18].

At fixed modifier content x and by focusing on the effect of sulfur content $m > 2$ larger than its stoichiometric value, one can probe the role of molecular flexibility since it is known that S-rich glasses belong to the flexible phase of rigidity theory [14–16]. Two starting configurations are used, ($m = 2$, $x = 9\%$, i.e., NS9) and ($m = 2$, $x = 50\%$, i.e., NS), corresponding to $N_{\mathrm{Na}} = 200$, $N_{\mathrm{Si}} = 900$, $N_S = 1900$, and $N_{\mathrm{Na}} = 1000$, $N_{\mathrm{Si}} = 500$, $N_S = 1500$, respectively, and one furthermore has, e.g., $m = (N\text{-}N_{\mathrm{Si}})/N_{\mathrm{Si}}$ for NS. The former system is stressed rigid [17,31] and according to the constraint count of Eq. (1), one expects the NS9 system to become flexible with increasing S at the MFRT point $m_c = 28/9 = 3.11$ or for $N_{\mathrm{Si}}^c = 9N/40 = 675$. The Na-rich system ($Na_2SiS_3$, NS) is already flexible [$f > 0$, Eq. (1)] and depolymerized [23] by the creation of NBS atoms (connected to Na ions), and one will check if an additional reduction of network connectivity could enhance even more the flexibility of the network in order to promote ion conduction. For both systems, with decreasing N_{Si} one acknowledges a decrease of the network connectivity (Fig. 2) which is characterized by the reduction of the average coordination number [18], consistent with the growth of flexible modes.

Focus is made on dynamic and electric properties. Figure 3(a) displays the calculated diffusivities D_k of the species k at different target temperatures as a function of the number of Si atoms N_{Si}. For NS9, the increase of flexibility (i.e., reduction of N_{Si}) obviously leads to a substantial increase of D_k which grows ($k = \mathrm{Na}$) from 0.06×10^{-5} cm^2 s^{-1} for $N = 850$ to 0.6×10^{-5} cm^2 s^{-1} for $N = 500$, and maximizes for all temperatures around $N_{\mathrm{Si}} \simeq 600$–$650$, i.e., close to the predicted MFRT threshold N_{Si}^c. Here one recognizes salient features associated with the well-established (waterlike) diffusivity anomaly in densified tetrahedral liquids (water, silica,…) for which network connectivity is controlled by the density induced coordination change [36]. Recently such dynamic anomalies have been unambiguously related with the isostatic character of tetrahedral liquids [37,38] which represents a stress-free state between the flexible and stressed rigid phase of glassy networks with changing connectedness. The temperature behavior leads to an obvious Arrhenius behavior $D_k(T) \propto \exp[-E_A/k_BT]$ and corresponding activation energies also display an anomaly with the flexibility index m (Fig. 4), the minimum in E_A being also a seminal signature of flexible to rigid transitions detected in early experiments [39] and up to recently [40]. Molecular simulation results, thus, indicate the presence of a MFRT signature for NS9. Results for the other system (NS) now clearly indicate, as expected, the absence of a MFRT with increasing flexibility index m since this system is already flexible for $m = 2$. This is confirmed by the absence of diffusivity anomalies at all considered temperatures, and instead, D_k grows continuously with m [18].

The ionic conductivity (σ) as a function of temperature T can be obtained from the Nernst-Einstein equation [41]:

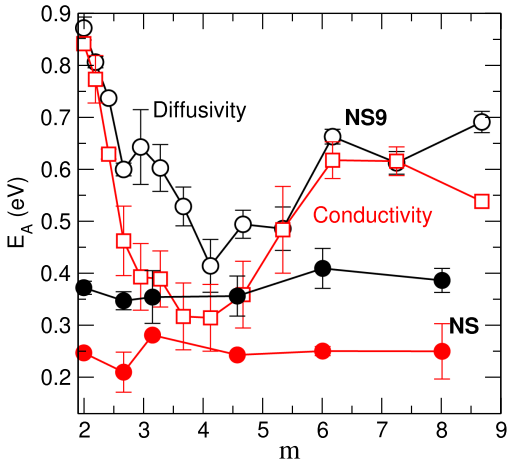

FIG. 4. Activation energy E_A for Na diffusivity (black) and conductivity (red) as a function of flexibility parameter m in NS9 (symbols) and NS (lines).

$$\sigma(T) = \lim_{t\to\infty} \frac{e^2}{6tVk_BT} \sum_{i,j} z_i z_j \langle [\mathbf{r}_i(t) - \mathbf{r}_i(0)][\mathbf{r}_j(t) - \mathbf{r}_j(0)] \rangle \tag{5}$$

where V is the volume of the simulation box, e is the elementary charge, and z_i and z_j are the fractional charges of ions i and j of the BM potential, respectively. Here $\mathbf{r}_i(t)$ is the position of atom i, and the brackets $\langle\rangle$ denote ensemble averages. Figure 3(b) now represents the system conductivity for different target temperatures as a function of the flexibility index m for both systems of interest, NS9 and NS. Here, one clearly acknowledges that the situation $m \geq 2$ induces a growth in σ by about one order of magnitude in NS9, and a marked jump occurs close to the locus $m_c = 3.11$ of the MFRT. For $m > m_c$, the reduction of σ is the consequence of the decrease of D_k in weakly connected systems [$N_{\mathrm{Si}} > 500$ in Fig. 3(a) or $m > 4.5$ in Fig. 3(b)], which in turn results from a reduction of excess entropy ($D \propto \exp[-A/TS_{ex}]$ [42]) driven by the profound structural modification of a loosely connected network, a feature not taken into account in the simple phenomenological model of Eq. (3). One also acknowledges a continuous increase of σ for the flexible NS system [Fig. 3(b)]. Similarly to the Na diffusivity, for NS9 the related activation energy obtained from an Arrhenius fit of the $\sigma(T)$ data also displays a minimum with the flexibility index m (Fig. 4) as a signature of a rigid to flexible transition, and not detected for the flexible NS liquid (red solid line).

The present results revealing the central role of network flexibility on electric properties in disordered media induce some broader perspectives, while also providing some clues for conductivity enhancement in a reasoned fashion. From a basic viewpoint, it highlights the generality of concepts from rigidity theory that obviously applies to the present complex glasses as well, as also recently emphasized for another complex material (calcium hydrates, cement [43]). Although, the trends from Fig. 1(d) (rigidity inspired calculation with varying x) and Fig. 3(b) (Kubo based calculation with varying m) cannot be directly compared, they lead to the same conclusion, i.e., flexibility and induced conductivity increase are achieved either by network depolymerization (as in archetypal silicates [13]) or by additional twofold atoms as suggested by the present numerical results. The obtained percolation of flexibility at $m = m_c$ can be put in perspective with the recent identification of percolation phenomena in Ag based sulfide electrolytes [5] where the substantial high ionic conductivity has been related to the formation of percolative channels with superionic conduction at a critical Ag content x_c. For the isochemical oxyde compound, calorimetric and scattering measurements have indicated that glasses satisfying $x > x_c$ belong to the flexible phase [44]. This provides direct experimental evidence that flexibility induces conductivity enhancement as it is here demonstrated that the addition of lower coordinated atoms brings into an amorphous network flexible deformation modes promoting the diffusion of charge carriers and conductivity. Finally, the fact that conductivity can be increased by an appropriate alloying should stimulate a new class of glassy materials in the context of all-solid-state battery applications: "off-stoichiometric network modified glasses." While such alloying methods can obviously not apply to silicates, sulfides are attractive because (i) they exhibit an increased conductivity ($10^{-3}\ \Omega^{-1}\,\mathrm{cm}^{-1}$) that results from the more polarizable sulfur atoms with respect to oxygen, and (ii) the flexibility index of sulfide network formers can be tuned continuously by compositional changes, from elemental sulfur to the stoichiometric compounds [32], in addition to the presence of alkali modifiers which disrupt the network by depolymerization. In this respect, identified target systems might use, e.g., GeS_4, SiS_3, or AsS_4 as network formers rather than the stoichiometric compounds GeS_2, SiS_2, or As_2S_3 [4].

Acknowledgments—The author acknowledges financial support from Chaire d'Excellence Sorbonne Université—Universidad Autónoma de Mexico, and from Fondation MAIF pour la recherche. Interactions and discussions with L.-M. Poitras, P. Boolchand, A. Piarristeguy, G. Naumis, H. Flores-Ruiz, and A. Pradel are also acknowledged.

[1] J.-M. Tarascon and M. Armand, Nature (London) **414**, 359 (2001).
[2] Z. A. Grady, C. J. Wilkinson, C. A. Randall, and J. C. Mauro, Front. Energy Res. **8**, 218 (2020).
[3] M. B. Isichenko, Rev. Mod. Phys. **64**, 961 (1992).
[4] M. Micoulaut, A. Piarristeguy, O. Masson, L.-M. Poitras, R. Escalier, A. Kachmar, and A. Pradel, Phys. Rev. B **108**, 144205 (2023).

[5] A. Qiao, J. Ren, H. Tao, X. Zhao, and Y. Yue, J. Phys. Chem. Lett. **13**, 10507 (2022).
[6] W. Dieterich and P. Maass, Z. Phys. Chem. **223**, 1187 (2009).
[7] W. Yao and S. W. Martin, Solid State Ionics **178**, 1777 (2008).
[8] A. Hayashi, K. Noi, A. Sakuda, and M. Tatsumisago, Nat. Commun. **3**, 856 (2012).
[9] Y. Seino, T. Ota, K. Takada, A. Hayashi, and M. Tatsumisago, Energy Environ. Sci. **7**, 627 (2014).
[10] J. H. Kennedy, Z. Zhang, and H. Eckert, J. Non-Cryst. Solids **123**, 328 (1990).
[11] P. Boolchand, P. Chen, and U. Vempati, J. Non-Cryst. Solids **355**, 1773 (2009).
[12] A. Pradel and A. PiarristeguyC. R. Géosci, C. R. Geosci. **354**, 79 (2022).
[13] M. Micoulaut, M. Malki, D. I. Novita, and P. Boolchand, Phys. Rev. B **80**, 184205 (2009).
[14] M. Micoulaut, Adv. Phys. X **1**, 147 (2016).
[15] P. K. Gupta and J. C. Mauro, J. Chem. Phys. **130**, 094503 (2009).
[16] M. M. Smedskjaer, J. C. Mauro, and Y. Yue, Phys. Rev. Lett. **105**, 115503 (2010).
[17] M. Zhang and P. Boolchand, Science **266**, 1355 (1994).
[18] See Supplemental Material at http://link.aps.org/supplemental/10.1103/PhysRevLett.134.036303 for model and numerical details, which includes the present Refs. and Refs. [18–28].
[19] M. Bauchy and M. Micoulaut, Eurphys. Lett. **104**, 56002 (2013).
[20] *Phase Transitions and Self-organization in Electronic and Molecular Networks*, edited by M. F. Thorpe and J. C. Phillips (Kluwer Academic/Plenum, New York, 2001).
[21] M. A. Brière, M. V. Chubynsky, and N. Mousseau, Phys. Rev. E **75**, 056108 (2007).
[22] L. Yan and M. Wyart, Phys. Rev. Lett. **113**, 215504 (2014).
[23] S. Sørensen, M. Smedskjaer, and M. Micoulaut, J. Phys. Chem. B **127**, 10179 (2023).
[24] M. Thomas, N. L. Peterson, and E. Hutchinson, J. Am. Ceram. Soc. **68**, 99 (1985).
[25] M. Ribes, B. Barrau, and J.-L. Souquet, J. Non-Cryst. Solids **38–39**, 271 (1980).
[26] D. E. Watson and S. W. Martin, J. Phys. Chem. B **122**, 10637 (2018).
[27] S. Chakraborty, P. Boolchand, and M. Micoulaut, Phys. Rev. B **96**, 094205 (2017).
[28] E. Bychkov, Solid State Ionics **136**, 1111 (2000).
[29] I. Alekseev, D. Fontanari, A. Sokolov, M. Bokova, M. Kassem, and E. Bychkov, *Ionic Conductivity and Tracer Diffusion in Glassy Chalcogenides* (World Scientific, Singapore, 2020).
[30] M. Micoulaut and J. C. Phillips, Phys. Rev. B **67**, 104204 (2003).
[31] Y. Vaills, T. Qu, M. Micoulaut, F. Chaimbault, and P. Boolchand, J. Phys. Condens. Matter **17**, 4889 (2005).
[32] S. Chakraborty and P. Boolchand, J. Phys. Chem. B **118**, 2249 (2014).
[33] W. A. Kamitakahara, R. L. Cappelletti, P. Boolchand, B. Halfpap, F. Gompf, D. A. Neumann, and H. Mutka, Phys. Rev. B **44**, 94 (1991).
[34] A. Dive, C. Benmore, M. Wilding, S. W. Martin, S. Beckman, and S. Banerjee, J. Phys. Chem. B **122**, 7597 (2018).
[35] D. E. Watson and S. W. Martin, J. Non-Cryst. Solids **471**, 39 (2017).
[36] J. Russo, K. Akahane, and H. Tanaka, Proc. Natl. Acad. Sci. U.S.A. **115**, E3333 (2018).
[37] M. Micoulaut and M. Bauchy, Phys. Rev. Lett. **118**, 145502 (2017).
[38] B. Mantisi, M. Bauchy, and M. Micoulaut, Phys. Rev. B **92**, 134201 (2015).
[39] M. Tatsumisago, B. L. Halfpap, J. L. Green, S. M. Lindsay, and C. A. Angell, Phys. Rev. Lett. **64**, 1549 (1990).
[40] A. Welton, R. Chbeir, M. McDonald, M. Burger, B. S. Almutairi, S. Chakravarty, and P. Boolchand, J. Phys. Chem. C **124**, 25087 (2020).
[41] J.-P. Hansen and I. R. McDonald, *Theory of Simple Liquids* (Academic Press, New York, 1988).
[42] Z. Yan, S. V. Buldyrev, and H. E. Stanley, Phys. Rev. E **78**, 051201 (2008).
[43] M. Bauchy, Mohammad Javad Abdolhosseini Qomi, C. Bichara, F.-J. Ulm, and Roland J.-M. Pellenq, Phys. Rev. Lett. **114**, 125502 (2015).
[44] D. I. Novita, P. Boolchand, M. Malki, and M. Micoulaut, J. Phys. Condens. Matter **21**, 205106 (2009).